# Catalytic Wet Air Oxidation of p-Coumaric Acid over Carbon Nanotubes and Activated Carbon

**ARTICLE** *in* INDUSTRIAL & ENGINEERING CHEMISTRY RESEARCH · JUNE 2011

Impact Factor: 2.59 · DOI: 10.1021/ie200492g



**6 AUTHORS**, INCLUDING:

Candida Milone
Università degli Studi di Messina
**109** PUBLICATIONS **2,242** CITATIONS
SEE PROFILE

Elpida Piperopoulos
Università degli Studi di Messina
**31** PUBLICATIONS **167** CITATIONS
SEE PROFILE

Saveria Santangelo
Mediterranean University of Reggio Calabria
**139** PUBLICATIONS **1,202** CITATIONS
SEE PROFILE

Signorino Galvagno
Università degli Studi di Messina
**184** PUBLICATIONS **4,581** CITATIONS
SEE PROFILE

I&EC research
Industrial & Engineering Chemistry Research

ARTICLE

pubs.acs.org/IECR

# Catalytic Wet Air Oxidation of *p*-Coumaric Acid over Carbon Nanotubes and Activated Carbon

Candida Milone,*[,†] Abdul Rahim Shahul Hameed,[†] Elpida Piperopoulos,[†] Saveria Santangelo,[‡] Maurizio Lanza,[§] and Signorino Galvagno[†]

[†]Department of Industrial Chemistry and Materials Engineering, Materials Engineering Section, University of Messina, Contrada di Dio 98166 Messina, Italy

[‡]Department of Mechanics and Materials, Engineering Faculty, "Mediterranea" University, Località Feo di Vito, 89122 Reggio Calabria, Italy

[§]CNR, Institute for Chemical Physical Processes, Messina Section, Viale Ferdinando Stagno d'Alcontres, 37 98158 Messina, Italy

**ABSTRACT:** The catalytic wet air oxidation of *p*-coumaric acid, a representative substrate of biorecalcitrant phenolic compounds typically found in olive oil processing wastewater, was carried out under mild conditions (in air at $T$ = 353 K and $P$ = 2 MPa) with activated carbon (AC) and multiwalled carbon nanotubes (CNTs). The influence of the CNT textural and surface chemistry modification, by oxidation with a nitric/sulfuric acid mixture, on the catalytic behavior was evaluated. AC and unoxidized CNTs showed the highest activity toward the degradation of *p*-coumaric acid and the highest efficiency toward total organic carbon (TOC) removal, which mainly occurs through mineralization to $CO_2$. As a result of oxidation with an acid mixture, the stability of the CNTs was dramatically worsened. From a comparison with literature data, it was concluded that the most efficient AC and unoxidized CNTs catalysts are, so far, very promising systems for *p*-coumaric acid degradation under mild conditions.

## 1. INTRODUCTION

Olive mill water (OMW) is an agro-industrial waste that is slightly acidic and is characterized by a high organic content.[1] The fraction of polyphenols that is present at high concentration (up to 2.5 g/L) leads to a serious concern for the direct biological treatment of OMW, owing to its high phytotoxicity and strong antimicrobial properties.[2,3] Pretreament methods suitable for the abatement of phenolic compounds are therefore needed. Several oxidation processes have been proposed for the abatement of biorecalcitrant phenolic compounds in OMW including catalytic ones that allow for a reduction of the severity of the oxidation conditions (pressure, temperature). Catalytic oxidation methods with homogeneous or heterogeneous catalysts and hydrogen peroxide as the oxidant, such the Fenton, photo-Fenton, and UV/$H_2O_2$ processes, have been extensively investigated,[4−6] whereas catalytic wet air oxidation (CWAO) processes are very limited,[7] although they use the less costly air as opposed to $H_2O_2$.

Aiming at the development of efficient catalysts for the CWAO of OMW, several studies have been published in the literature that deal with the oxidation of *p*-coumaric acid [3-(4-hydroxyphenyl)-2-propenoic acid],[7−12] which is closely related by chemical structure to the other compounds of the OMW polyphenolic fraction. Heterogeneous catalysts are always preferred to homogeneous ones, so that further treatments for catalyst removal from the water stream can be avoided.

Although a direct comparison of literature data is somewhat difficult to be done because of differences in operating conditions (catalyst concentration, air pressure, and temperature), the main results reported for the CWAO of *p*-coumaric acid are reported herein. Cobalt/bismuth oxide composites and CuO−ZnO/$Al_2O_3$ are effective in the oxidation of *p*-coumaric acid at 2.8 MPa and 403 K, with the almost-complete destruction of the acid after 10 min of reaction and a TOC abatement of 55% for CuO−ZnO/$Al_2O_3$ and 66% for Co/Bi catalyst.[8] A strong drawback of these systems is the significant leaching of $Co^{2+}$ and $Cu^{2+}$ ions in the water stream. Neri et al.[9] investigated the catalytic activity of pure metal oxides such as $Fe_2O_3$, ZnO, and $CeO_2$ and mixed iron−cerium and zinc−cerium oxides in the CWAO of *p*-coumaric acid ($P$ = 2 MPa, $T$ = 353−403 K), showing that $Fe_2O_3$−$CeO_2$ mixed oxides present the highest oxidation rate of *p*-coumaric acid with a TOC removal of 90% after 5 min of reaction.

The CWAO of *p*-coumaric acid over Pt and Ru supported on $ZrO_2$ and $TiO_2$ ($P$ = 5 MPa, $T$ = 413 K) occurs at a higher rate with catalysts prepared by ultrasound irradiation than by impregnation because of the higher dispersion of the active metal.[10] Among catalysts prepared by impregnation, Ru-based systems are more active than Pt-based ones.[10] TOC removals of 80% and 90% after 400 min of reaction were achieved with 3% Ru supported on $TiO_2$ and $ZrO_2$, respectively, whereas with Pt-based catalysts having the same metal load, the maximum TOC abatement was 60% with $TiO_2$ as the support.[11] On the most active Ru catalysts, the removal of organic carbon from the solution is mainly due to mineralization to $CO_2$ (∼70% of initial TOC), whereas a minor contribution is given by adsorption on the catalyst surface.[11]

Pt supported on $CeO_2$ catalysts allow a high TOC removal (∼90%) to be achieved already after a residence time of 300 min in the oxidation of *p*-coumaric acid at $P$ = 2 MPa and $T$ = 353 K with a mineralization of 55% of the initial carbon content.[12]

**Received:** March 11, 2011
**Accepted:** June 18, 2011
**Revised:** May 24, 2011
**Published:** June 18, 2011





dx.doi.org/10.1021/ie200492g | *Ind. Eng. Chem. Res.* 2011, 50, 9043–9053

Table 1. Sample Codes, Nitric/Sulfuric Acid Mixture Volume Ratios Used for CNT Oxidation, Ash Contents (wt %), Surface Areas of Fresh (SA) and Spent ($SA_{AR}$) Catalysts, and Results of Raman Spectra Decompositions $I_G/I_D$, $I_{G'}/I_G$, and $I_{G'}/I_D$ Indicating the G/D, G′/G, and G′/D Intensity Ratios

| sample | nitric/sulfuric (v/v) | ash (wt %) | SA ($m^2/g$) | $SA_{AR}$ ($m^2/g$) | $I_G/I_D$ | $I_{G'}/I_G$ | $I_{G'}/I_D$ |
|---|---|---|---|---|---|---|---|
| AC | – | 0.4 | 631 | 220 | nd[a] | nd | nd |
| p-CNTs | – | 5.9 | 196 | 154 | 0.56 | 0.82 | 0.46 |
| $f_{3:1}$-CNTs | 3:1 | 5.5 | 195 | 152 | 0.54 | 0.58 | 0.31 |
| $f_{1:1}$-CNTs | 1:1 | 4.8 | 194 | 155 | 0.48 | 0.50 | 0.24 |
| $f_{1:3}$-CNTs | 1:3 | 3.4 | 172 | 138 | 0.47 | 0.49 | 0.23 |

[a] nd = not determined.

The aim of this work was the evaluation of the feasibility of carbon catalysts such as AC and CNTs for the CWAO of *p*-coumaric acid. These materials, because of their remarkable performance with respect to metal or oxide catalysts, are finding an increasing number of applications as catalysts on their own, including in CWAO.[13−23] Given that the catalytic activity of a carbonaceous material is determined by the nature, concentration, and accessibility of its active sites, it is obviously somewhat related to the material's texture. However, a decisive effect on the catalytic properties is exerted by the surface chemistry.[19,21−26]

In the present work, the results of the CWAO of *p*-coumaric acid at $P = 2$ MPa and $T = 353$ K with commercial AC and CNTs synthesized by the catalytic chemical vapor deposition (CCVD) of isobutane[27] are discussed.

The influence of CNT textural and surface modifications, upon oxidation with a nitric/sulfuric acid mixture at different volume ratios, as monitored by transmission electron microscopy (TEM), Raman spectroscopy (RS), and temperature-programmed desorption (TPD), on the catalytic behavior in the degradation of *p*-coumaric acid is reported.

## 2. EXPERIMENTAL SECTION

**2.1. Materials.** AC was supplied by Carlo Erba (CAS 7440-44-0). CNTs were prepared by the CCVD of isobutane (*i*-$C_4H_{10}$) over Fe supported on $Al_2O_3$ catalyst (iron loading = 29 wt %).[27]

CCVD synthesis was carried out placing the catalyst (0.5 g) in a quartz boat inside a quartz tube located in a horizontal electric furnace. The catalyst was reduced at 773 K under a flow of hydrogen/helium; after 1 h, the temperature was raised to 873 K, and then the helium was replaced by isobutane. The $H_2$/*i*-$C_4H_{10}$ volume ratio was 1:1, and the total flow was kept at 120 sccm for 2 h. After synthesis, the product was cooled to room temperature under a helium atmosphere.

The product was treated with a solution of NaOH (1 M) at 353 K to remove the support and then with a solution of HCl (1 M) to remove the iron particles. The purified sample (p-CNTs) was finally washed with distilled water and dried at 353 K for 12 h.

Oxidation of p-CNTs in a nitric/sulfuric acid mixture was undertaken in an ultrasonic bath at 333 K for 6 h. A 3-g sample of p-CNTs was weighed and added to 300 mL of acid mixture (67% $HNO_3$ and 98% $H_2SO_4$) having a proper volume ratio. Mixtures with three different nitric/sulfuric acid volume ratios were used: 3:1, 1:1, and 1:3.

After treatment, the carbon material was separated by filtration through 0.2-$\mu$m filter paper, washed with water to neutral pH, and dried at 353 K for 12 h.

Table 1 reports the sample codes of the catalysts. For CNTs, the catalyst code summarizes information related to their treatment. (p-CNTs stands for purified CNTs, and $f_{N:S}$-CNTs stands for oxidized CNTs. The subscript N:S indicates the nitric/sulfuric volume ratio used for the oxidation).

**2.2. Catalyst Characterization.** The amount of ash (wt %) from the carbonaceous materials was evaluated by measuring the residual weight upon combustion of a known amount of sample in excess $O_2$ at 1073 K, a temperature largely exceeding the range of temperatures at which the most oxidation-resistant CNTs burn.[27]

Surface areas ($m^2/g$) was determined by adsorption−desorption of dinitrogen at 77 K, after the samples had been outgassed ($10^{-4}$ mbar) at 353 K for 2 h, using Qsurf Series surface area analyzers.

The morphologies and dimensions of the CNTs were investigated by using a JEOL JEM 2010 TEM instrument, operating at 200 kV and equipped with a Gatan 794 Multi-Scan CCD camera. The nanotubes were dispersed in isopropanol and deposited on a grid covered with holey carbon film.

RS analysis was carried out, at room temperature, in the 800−3350 $cm^{-1}$ spectral range by using a double monochromator (Jobin Yvon Ramanor U-1000) equipped with a microscope (Olympus BX40) and a photomultiplier (Hamamatsu R943-02) operating in photon-counting mode. An $Ar^+$ laser (Coherent Innova 70) operating at 2.41 eV (514.5 nm) excited Raman scattering.

Light was focused onto the sample to a spot of 2-$\mu$m diameter through the X50 microscope objective lens. To prevent annealing effects, the power at the sample surface was kept at 3 mW. The thus-obtained power density ($<1 \times 10^5$ W/$cm^2$) was smaller than that used by other groups.[28,29]

A 30-s acquisition time was used to improve the signal-to-noise ratio. To reliably describe the sample bulk, several different locations of each specimen were sampled on account of the possible structural inhomogeneity.

After normalization and averaging, the background was subtracted, and Lorentzian bands were used to reproduce the spectra. The integrated intensity ratios were then calculated.

TPD measurements were carried out using a flow reactor equipped with a quadrupole mass spectrometer (HPR 20 Hiden Analytical instrument). Samples (30 mg) were placed in a U-shaped quartz tube inside an electrical furnace and heated at 10 K $min^{-1}$ to 1373 K under a constant flow rate of helium (30 sccm). The mass signals $m/z = 28$ (CO), 30 (NO), 44 ($CO_2$), and 64 ($SO_2$) were monitored during the analysis. The amounts of CO, $CO_2$, NO, and $SO_2$ were calibrated at the end of each analysis with pure gases. After treatment of the acquired data, the TPD spectra of CO, $CO_2$, NO, and $SO_2$ (in $\mu$mol $g^{-1}$ $s^{-1}$) were obtained.

The material pH at the point zero charge, $pH_{pzc}$, was also determined by using a drift method described elsewhere.[30,31]


dx.doi.org/10.1021/ie200492g |*Ind. Eng. Chem. Res.* 2011, 50, 9043–9053

**2.3. *p*-Coumaric Acid Oxidation Procedure.** The reaction was carried out in an autoclave (Parr model 4560) equipped with a magnetically driven stirrer at 353 K, in air at $P$ = 2 MPa. The pressure was maintained throughout the experiment by connecting the autoclave to an air cylinder. The reaction vessel and all internal parts in contact with the reaction mixture were made of Teflon to avoid metal contamination.

To minimize dead reaction time due to heating, the catalyst (0.5 g) was soaked in 100 mL of water, and the temperature was increased to 353 K. Then, 25 mL of *p*-coumaric acid aqueous solution was introduced into the reaction vessel through the gas entrance tube.

The *p*-coumaric acid concentration in the reactor was 4.5 mM, corresponding to the maximum solubility of *p*-coumaric acid in water at 298 K. Liquid samples were periodically withdrawn from the reactor and analyzed with high-performance liquid chromatograph (Agilent 1100 series) equipped with a Symmetry C18 column (4.6 mm × 250 mm) and a photodiode array detector (PAD).

The calibration curve for the reagent was obtained by analyzing the reference sample under the above-reported experimental conditions.

The total organic carbon content in the solution was determined with a Shimadzu 5050 TOC analyzer.

The amount of carbon removed by adsorption onto the catalysts was evaluated by temperature-programmed oxidation (TPO) as the difference between the amounts of $CO_2$ evolved during the combustion of the used and fresh catalysts. Used catalysts were recovered after the reaction by filtration, washed with cold water, and dried under a vacuum at 353 K for 3 h.

TPO experiments were carried out under the range of temperature from 298 to 1273 K, at a heating rate 10 K $min^{-1}$, and in the presence of a large excess of $O_2$, 20 sccm of 4% $O_2$/He (vol.%), to favor the complete carbon combustion. $C_{ads}$ (%) was calculated as

$$C_{ads}\ (\%) = \frac{\left(\frac{\mathrm{mol}_{CO_2(AR)} \times \mathrm{wt}_{cat}}{\mathrm{wt}_{(AR)}}\right) - \left(\frac{\mathrm{mol}_{CO_2(FC)} \times \mathrm{wt}_{cat}}{\mathrm{wt}_{(FC)}}\right)}{C_{init}} \times 100$$

where $\mathrm{mol}_{CO_2(AR)}$ and $\mathrm{mol}_{CO_2(FC)}$ are the numbers of moles of $CO_2$ measured from the TPO analysis of the used (AR) and fresh (FC) catalysts; $\mathrm{wt}_{cat}$ is the weight (g) of catalyst used in the reaction; $\mathrm{wt}_{(AR)}$ and $\mathrm{wt}_{(FC)}$ represent the weight of the used and fresh catalysts, respectively, as analyzed by TPO; $C_{init}$ represents the number of moles of C introduced into the reaction vessel at beginning of the reaction.

The rate of removal of *p*-coumaric acid ($V$, mol $g_{cat}^{-1}$ $min^{-1}$) was calculated as

$$V = \frac{\mathrm{mol}_{PCA(t_0)}\left(1 - \frac{C_t}{C_o}\right)}{g_{cat}\, t}$$

where $\mathrm{mol}_{PCA(t_0)}$ represents the amount of reagent ($5.6 \times 10^{-4}$ mol), $C_t/C_0$ represents the fraction of the reagent detected at time $t$, $g_{cat}$ is the amount of catalyst, and $t$ is the reaction time (min).

## 3. RESULTS AND DISCUSSION

**3.1. Characterization of Catalysts.** Table 1 shows that the carbonaceous materials investigated had rather different ash contents: AC and p-CNTs had the lowest and highest residual amounts upon combustion, 0.4 and 5.9 wt %, respectively. The CNT liquid-phase treatment in 3:1 nitric/sulfuric acid mixture caused a slight decrease of the ash content to 5.5 wt %. As the sulfuric acid concentration increased, the ash content further diminished, reaching the lowest value (3.4 wt %) in the $f_{1:3}$-CNTs sample. The residue obtained upon CNT oxidation, which appeared reddish colored, was iron oxide originating from the oxidation of iron metal catalyst encapsulated by the graphitic structures during CCVD synthesis,[32] as shown by TEM (Figure 1a), that was rather difficult to dissolve under the mild post synthesis purification with 1 M HCl. The absence of aluminum in the residue, confirmed by analysis of the solution obtained upon contacting the solid with NaOH by means of atomic adsorption spectrometry, indicates the complete elimination of catalyst support ($Al_2O_3$) from the carbonaceous materials.

In terms of surface area (SA), measured by $N_2$ adsorption and reported in Table 1, the highest value (631 $m^2/g$) was found for AC; p-CNTs showed a lower but still notable SA (196 $m^2/g$). Oxidative treatment with nitric/sulfuric acid mixtures ($f_{N:S}$-CNTs samples) did not significantly modify the SA with respect to that of p-CNTs. Instead, very similar values were found for p-CNTs, $f_{3:1}$-CNTs, and $f_{1:1}$-CNTs, and a slight reduction, by 13%, was observed at the highest sulfuric acid concentration ($f_{1:3}$-CNTs sample).

TEM analysis of p-CNTs and $f_{N:S}$-CNTs, displayed in Figures 1 and 2, shows the structural modification that occurred upon oxidation.

Figure 1b shows that p-CNTs formed long highly entangled carbon filaments (length ≥ 5 $\mu$m, as shown in the inset of Figure 1b) with external diameters between 5 and 20 nm. Higher-magnification images demonstrate that the p-CNT walls mainly consist of smooth graphene layers (Figure 2a). Upon oxidation with the 3:1 nitric/sulfuric acid mixture, no considerable modification of the side graphitic sheets occurred (Figure 2b). Instead, because the concentration of sulfuric acid increased, the sidewalls also degraded, so that edges and steps at external sheets were clearly visible (Figure 2c). These results undoubtedly indicate that the use of sulfuric acid-rich mixtures is more harmful for the CNT crystalline structure, although it is worth noting that, even under that most aggressive oxidation conditions, the tubular structure of the carbonaceous material was preserved (Figure 1c−e) and no other carbon structures, such as amorphous carbon and/or graphite platelets, formed. As a result of oxidation with the nitric/sulfuric acid mixture, a reduction of the CNT length, especially for the most degraded $f_{1:3}$-CNTs, was also observed, as shown in the inset of Figure 1e, where filaments (≤3 $\mu$m) shorter than p-CNTs are also visible.

The CNT breakage induced by the use of the most powerful oxidant mixture would account for the evident decrease of the residual iron content in the $f_{1:3}$-CNTs (Table 1) compared to the p-CNTs. Indeed, the creation of access points inside the nanotubes where encapsulated iron catalyst was located would allow the penetration of the acid solution, thereby enhancing its dissolution.

The SAs, instead, seem to be inconsistent with CNT modification as depicted by TEM. Indeed, because of the rupture of the nanotubes, their inner side should also become accessible for $N_2$ molecules, in which case an SA increase would be expected, rather than a decrease as in the case of $f_{1:3}$-CNTs (Table 1).

A possible rationalization of the experimental evidence takes into account the occurrence of two opposite effects: (1) SA

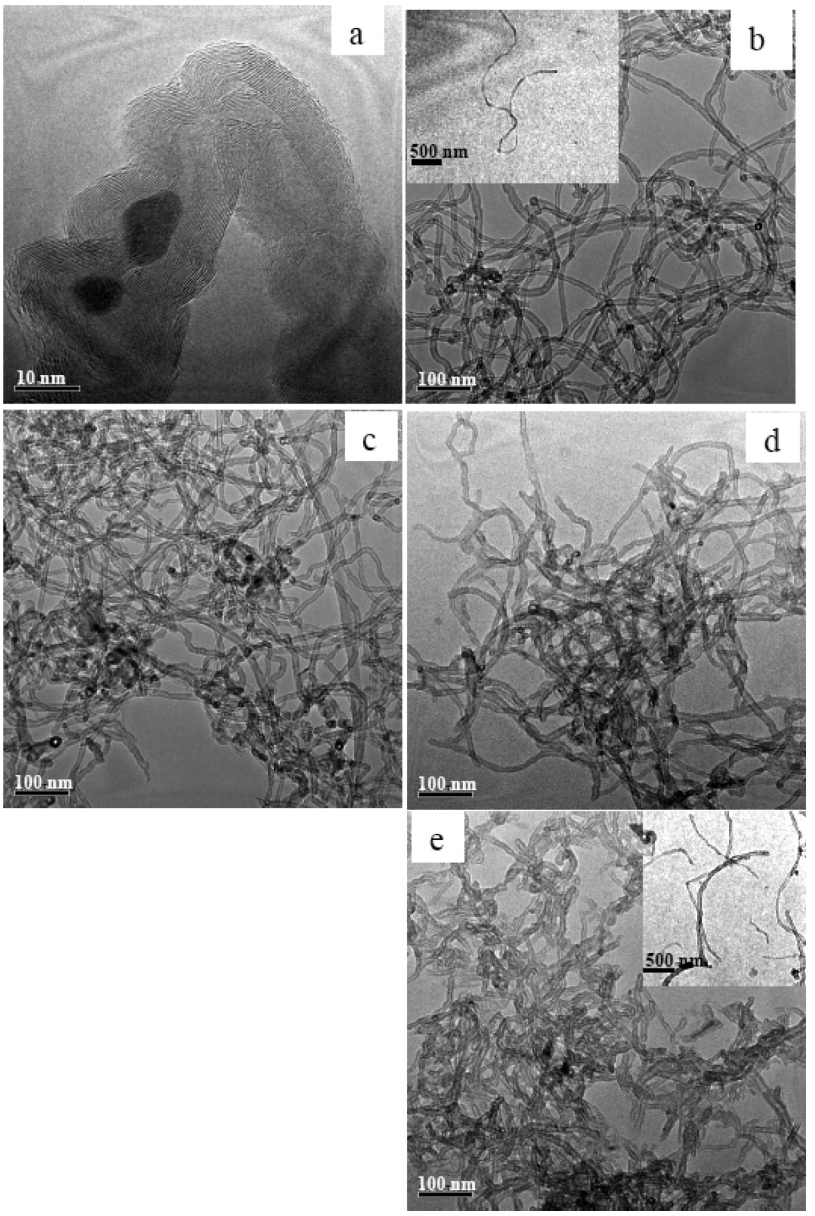


**Figure 1.** Morphologies of purified and acid-treated CNTs as monitored by TEM: (a) iron inclusion, (b) p-CNTs, (c) $f_{3:1}$-CNTs, (d) $f_{1:1}$-CNTs, and (e) $f_{1:3}$-CNTs.

increase because of the contribution of the internal surface owing to tube breakage and (2) SA decrease because of the stronger electrostatic interaction between the polar functional groups introduced,[21,33,34] which reduces the tube−tube distance and hence the exposed external surface area. It is indeed known that strong CNT agglomeration occurs upon oxidative treatment.[35]

The measured SAs might, therefore, be the result of these opposite effects, and the contribution of each should be strongly dependent on the oxidation conditions and, this, on the extent of tube opening and/or breaking and the amount of polar groups introduced. This hypothesis could also account for the controversial data present in the literature.[21,33]

The progressive degradation of the CNT structure, obtained by lowering the nitric/sulfuric volume ratio, was also confirmed by RS, a technique that is also widely used to check the effectiveness of the acid treatment on CNTs.[36−38]

Figure 3 compares the spectra measured on p-CNTs and $f_{N:S}$-CNTs and shows that all of the samples exhibited similar Raman features: the graphite-like in-plane optical mode at 1580 $cm^{-1}$ (G-band); the band at 1350 $cm^{-1}$ originating from lattice defects (vacancies, pentagons, heptagons, or other defects and by finite-size effects) that break the basic graphene layer symmetry (D-band);[39,40] its overtone at 2700 $cm^{-1}$ (G′-band) that, conversely, is detected only in nanotubes consisting of sequences of smooth graphene sheets[41] (i.e., in the presence of graphitic long-range order); and the D′-band mode at 1610 $cm^{-1}$ that, similar to the D-band mode, is a disorder-activated double-resonance Raman feature, with the two modes originating from inter- and intravalley scattering processes, respectively.[42]

After background subtraction, the spectral features were fitted to Lorentzian bands, and the integrated-intensity ratios were calculated. The extent of structural defects was monitored by the

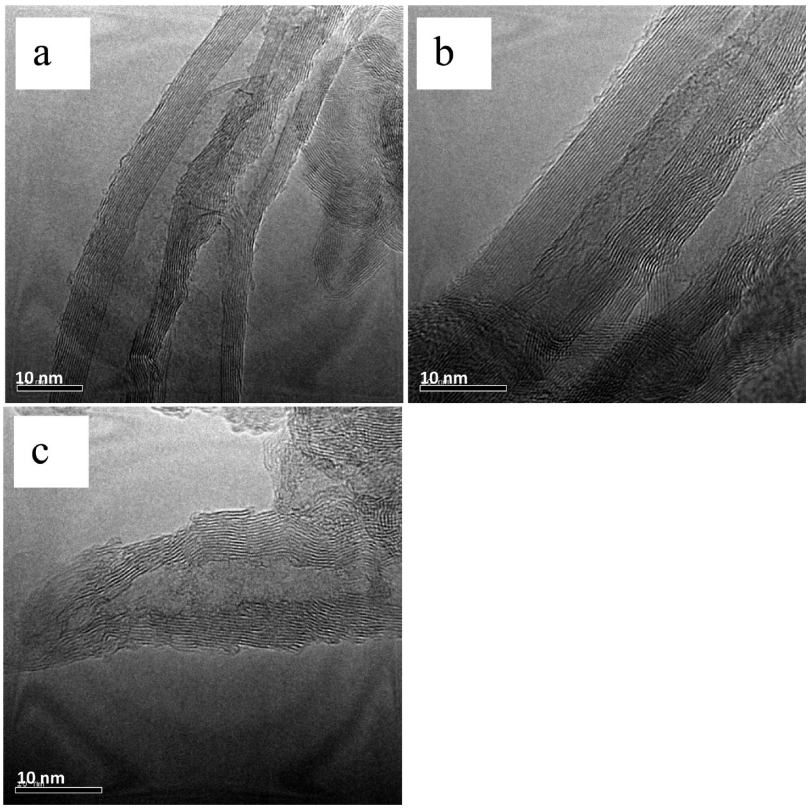


**Figure 2.** Effect of the nitric/sulfuric acid volume ratio on the degradation of CNTs, as monitored by TEM: (a) p-CNTs, (b) $f_{3:1}$-CNTs, and (c) $f_{1:3}$-CNTs.

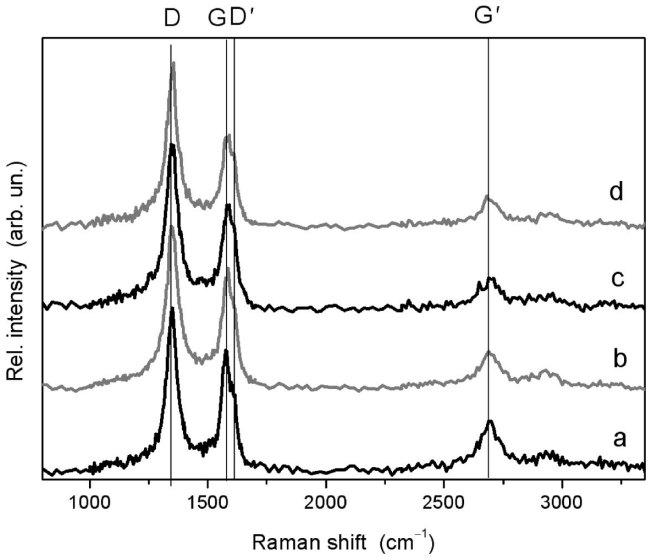


**Figure 3.** Effect of the nitric/sulfuric acid volume ratio on the crystalline structure of CNTs, as monitored by Raman spectroscopy (spectra normalized to the D-band intensity): (a) p-CNTs, (b) $f_{3:1}$-CNTs, (c) $f_{1:1}$-CNTs, and (d) $f_{1:3}$-CNTs.

G/D intensity ratio ($I_G/I_D$)[41] that, for fixed excitation energy, decreases with decreasing in-plane correlation length (i.e., mean interdefect distance[39,43]). Instead, the G′/G intensity ratio ($I_{G'}/I_G$) is generally regarded as an indicator of long-range order.[41] Thus, the overall crystalline quality, which improves with increasing mean interdefect distance and/or ununulated tube-wall number (i.e., with increasing G/D and/or G′/G ratios, respectively), is pictorially described by the G′/D intensity ratio ($I_{G'}/I_D$).[44]

The results, shown in Table 1, confirm that acid attack increased the density of lattice defects, as signaled by the lowering of $I_G/I_D$, and downgraded the CNT crystalline quality, as evidenced by the lowering of $I_{G'}/I_D$.

The lowering of the Raman indicators $I_G/I_D$ and $I_{G'}/I_D$ became more pronounced as the nitric/sulfuric acid volume ratio decreased, indicating that, with sulfuric acid-rich mixtures, the oxidation conditions become more harmful to the CNT crystallinity, in agreement with TEM analysis.

The acid/base character of the carbonaceous samples was evaluated by means of the TPD monitoring of the CO ($m/e$ = 28) and $CO_2$ ($m/e$ = 44) molecules resulting from the decomposition of various oxygen-containing groups such as carboxyl, carbonyl, phenol, and lactones present on and/or introduced upon oxidation onto the carbon surfaces. In particular, the $CO/CO_2$ ratio can be taken as an indicator of the acid/base character of carbonaceous materials with an increase of the $CO/CO_2$ ratio indicating an enhancement of the basic nature.[45−48] In addition to CO and $CO_2$, the evolutions of NO ($m/e$ = 30) and $SO_2$ ($m/e$ = 64) molecules, were monitored for all samples.

TPD spectra are shown in Figure 4 and the corresponding concentrations of the monitored species are gathered in Table 2, allowing for a comparison of the total amounts of functional groups present on AC and p-CNTs and introduced onto the surfaces of the CNT samples subjected to the acid

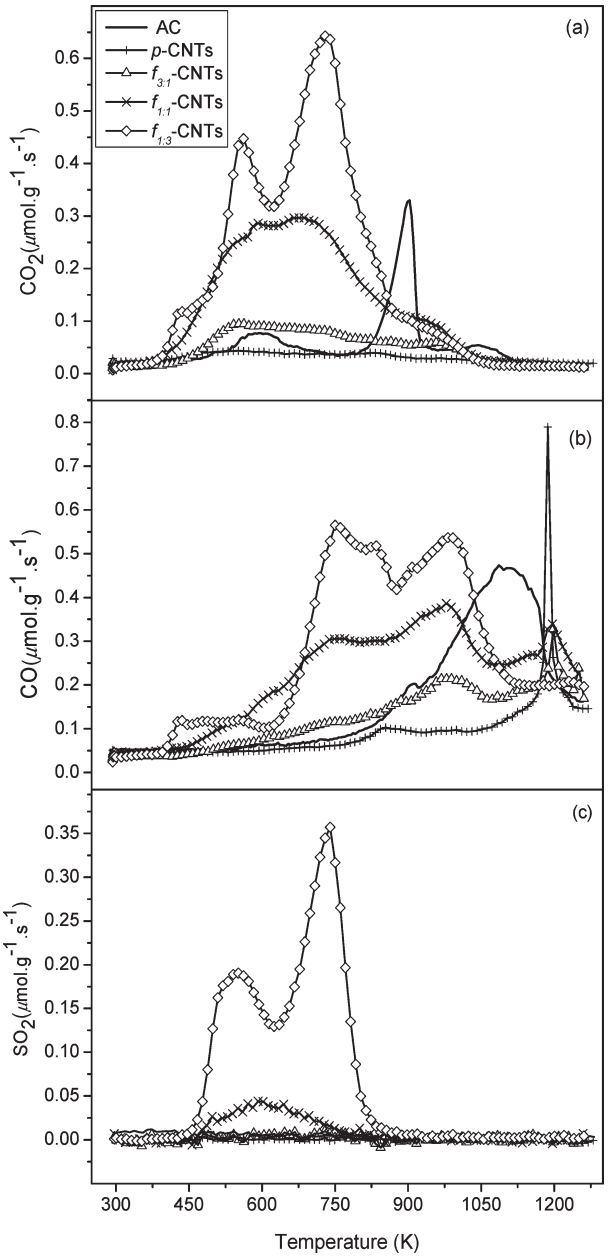


**Figure 4.** TPD profiles of AC, p-CNTs, and $f_{N:S}$-CNTs samples: (a) $CO_2$, (b) CO, and (c) $SO_2$.

treatments. The TPD results also allow for the identification and quantification of the functional groups present on the material surface by peak assignment, as described elsewhere.[26,30,49,50]

Figure 4a shows that AC releases $CO_2$ at lower (480−650 K) and high (800−900 K) temperature, which agrees well with the decompositions of carboxylic acid groups and lactones, respectively.[26,30] CO evolution (Figure 4b) occurred over a wide range of temperatures (800−1290 K) because of the decomposition of phenols (837−1023 K)[26,30] and carbonyls/quinones at higher temperature (973−1223 K);[26,30] the maximum desorption rate at ∼1080 K suggests that the main contribution to CO evolution was made by the most stable carbonyl-type functional groups. In contrast, p-CNTs exhibited only a broad and low-intensity $CO_2$ peak (400−650 K) and a sharp CO peak at ∼1200 K likely arising from the more energy-demanding decomposition of carbonyl/quinone groups[26,30] (Figure 4b).

Upon CNT oxidation with nitric/sulfuric acid mixtures, $CO_2$ and CO evolution increased with increasing sulfuric acid concentration, as shown in Table 2, indicating an enhancement of the functional groups introduced onto the CNT surface as the oxidative conditions became more powerful. Figure 4a shows that $CO_2$ was released from $f_{N:S}$-CNTs over a broad range of temperatures (400−1000 K), suggesting that different functionalities such as carboxylic acid, carboxylic anhydrides, and lactones were introduced. The amount of $CO_2$ released was more abundant for the samples obtained upon oxidation with sulfuric acid-rich mixtures (i.e., $f_{1:1}$-CNTs and $f_{1:3}$-CNTs); the range of temperatures over which the main desorption occurred (450−873 K) suggests that carboxylic acids and anhydride functional groups were prevalently added onto the surface.

CO desorption profiles, as shown in Figure 4b, also increased and broadened because of the overlap of different contributions such as carboxylic anhydride groups, occurring between 723−900 K, where CO and $CO_2$ partly appear, and phenols (873−1023 K).[26,30] The sharp CO peak present in the p-CNTs profile at ∼1200 K decreased for $f_{3:1}$-CNTs and $f_{1:1}$-CNTs and disappeared on the more oxidized $f_{1:3}$-CNTs, likely because of the destruction of carbonyl/quinone functionalities likely due to overoxidation.

NO release (not shown) occurred only to a very low extent (Table 2) in the range of temperature 400−600 K for all samples investigated, except p-CNTs.

Similarly, the evolution of $SO_2$ (Figure 4c) was evident for all samples except p-CNTs; AC and $f_{3:1}$-CNTs released the lowest amounts of $SO_2$, and the most oxidized samples, $f_{1:1}$-CNTs and $f_{1:3}$-CNTs, released more, in line with the increase of the sulfuric acid concentration in the oxidant mixture (Table 2). The range of temperatures over which $SO_2$ release occurred, 450−800 K, agrees with the decomposition of thiol and sulfonic acid groups.[51,52]

From the $CO/CO_2$ ratios reported in Table 2, it appears that AC and p-CNTs exhibited higher base characters (i.e., higher ratios); as a result of p-CNTs oxidation, the acid character of the resulting materials was enhanced, as shown by the lowering of $CO/CO_2$ ratio. These observations are consistent with the measured $pH_{pzc}$ values (Table 2).

The fact that the $pH_{pzc}$ of AC was measured to be higher than that of p-CNTs is due to the presence of a higher amount of basic carbonyl-type groups, as suggested by the highest amount of evolved CO for AC (Table 2) mainly occurring at $T > 973$ K (Figure 4b). The acid treatment of CNTs strongly enhanced their acidity, and the $pH_{pzc}$ decreased from 7.0 in the case of p-CNTs to 2.5 for $f_{3:1}$-CNTs, in agreement with previous findings for acid-treated carbon nanotubes.[30] A further lowering of $pH_{pzc}$ was observed upon treatment with more sulfuric acid-rich mixtures (samples $f_{1:1}$-CNTs and $f_{1:3}$-CNTs in Table 2), because of the more pronounced increase of acidic carboxylic groups and anhydrides, as shown by the $CO_2$ evolution in the range 400−800 K in Figure 4a, and phenols, as shown by the CO evolution in the range 873−1023 K in Figure 4a, with respect to the basic carbonyl groups monitored by CO evolution at $T > 973$ K in Figure 4b. In addition, it should be considered that the increase in sulfur groups also contributed to the lowering of $pH_{pzc}$, as thiol and sulfonic acid are moderately and strongly acidic, respectively.

**3.2. Degradation of *p*-Coumaric Acid.** The CWAO of *p*-coumaric acid was carried out in air at $T = 353$ K and $P = 2$ MPa.

Table 2. Concentrations ($\mu$mol $g_{cat}^{-1}$) of CO, $CO_2$, NO, and $SO_2$ Released during TPD of Carbon Materials; pH Values at the Point Zero Charge, Removal Rates of *p*-Coumaric Acid ($V$, mol $g_{cat}^{-1}$ $min^{-1}$), Removal Rates upon Subtraction of the Adsorption Contribution ($V - V_{ads}$), Amounts of Carbon Removed by Adsorption ($C_{ads}$, %), and Mineralization Effectiveness Values ($C_{CO_2}$, %)

| catalyst | $CO_2$ ($\mu$mol $g_{cat}^{-1}$) | CO ($\mu$mol $g_{cat}^{-1}$) | NO ($\mu$mol $g_{cat}^{-1}$) | $SO_2$ ($\mu$mol $g_{cat}^{-1}$) | $CO/CO_2$ | $pH_{pzc}$ | $V$ (mol $g_{cat}^{-1}$ $min^{-1}$) $10^5$ | $V - V_{ads}$[a] (mol $g_{cat}^{-1}$ $min^{-1}$) $10^5$ | $C_{ads}$ (%) | $C_{CO_2}$ (%) |
|---|---|---|---|---|---|---|---|---|---|---|
| AC | 139 | 670 | 3 | 7 | 4.8 | 10.02 | 3.4 | 2.9 | 14.1 | 71.2 |
| p-CNTs | 75 | 330 | – | – | 4.4 | 7.01 | 2.3 | 2.1 | 5.0 | 82.6 |
| $f_{3:1}$-CNTs | 244 | 660 | 3 | 6 | 2.7 | 2.54 | 1.5 | 1.3 | 5.3 | 52.0 |
| $f_{1:1}$-CNTs | 737 | 1280 | 4 | 182 | 1.7 | 2.32 | 1.2 | 1.0 | 5.0 | 54.7 |
| $f_{1:3}$-CNTs | 1140 | 1490 | 2 | 448 | 1.3 | 2.00 | 2.1 | 2.0 | 3.0 | 21.9 |

[a] Calculated as $[mol_{PCA(t_0)} \times C_{ads}(\%)]/[g_{cat} \times t\,(min) \times 100]$, where $mol_{PCA(t_0)} = 5.6 \times 10^{-4}$, $g_{cat} = 0.5$ g, and $t = 30$ min

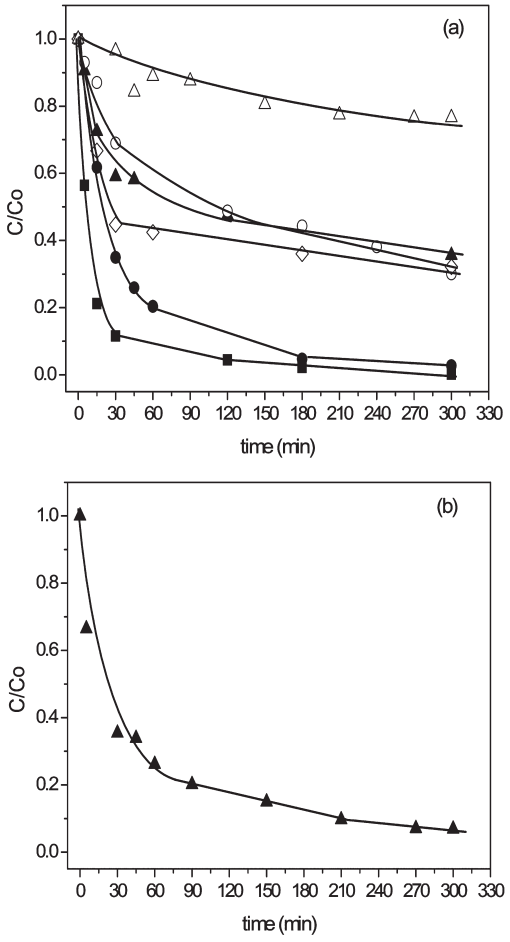


**Figure 5.** (a) *p*-Coumaric acid profile versus contact time during CWAO at 353 K in air at 2 MPa: (■) AC, (●) p-CNTs, (▲) $f_{3:1}$-CNTs, (○) $f_{1:1}$-CNTs, (◊) $f_{1:3}$-CNTs, (Δ) no catalyst. (b) $f_{3:1}$-CNTs treated at 873 K for 1 h under 30 sccm of He.

Figure 5a shows *p*-coumaric acid removal ($C/C_0$) as a function of contact time, also in the absence of catalyst. Among the samples investigated, AC and p-CNTs almost completely eliminated the organic compound from the solution after 5 h, whereas in the presence of $f_{N:S}$-CNTs, only 60% of the *p*-coumaric acid disappeared. However, this value was higher than the 20% reached, at the same contact time, during the oxidation of *p*-coumaric acid in the absence of a catalyst.

Figure 5a also shows that $f_{N:S}$-CNTs underwent a rapid deactivation during reaction. Indeed, within 30 min of reaction, the disappearance of *p*-coumaric acid occurred at a higher rate, and it significantly decreased with increasing contact time.

Table 2 reports the amount of organic carbon removed by adsorption onto the catalyst surface compared to the initial amount introduced into the reaction vessel, $C_{ads}$ (%), evaluated by TPO analysis as described in section 2.3. $C_{ads}$ (%) was found to be significantly higher for AC than for p-CNTs.

The modification of the surface groups of the CNTs upon oxidation (samples $f_{3:1}$-CNTs, and $f_{1:1}$-CNTs) did not significantly modify their adsorption capacity (Table 2) with respect to that of the pristine CNTs; a lowering of $C_{ads}$ was observed only for the most oxidized $f_{1:3}$-CNTs. The surface area analysis of the spent catalyst ($SA_{AR}$) recovered after one catalytic cycle and reported in Table 1 shows that AC suffered the highest loss (~65%) whereas, for all of the CNT samples, the loss occurred to a lower extent (~20%). These results agree with the differences in the $C_{ads}$ values and suggest that, in the case of AC, a strongest pore blockage occurs. The adsorption capacity of the investigated samples substantially reflects the changes in the SA (Table 1). However, effects other than merely adsorption might have occurred. Indeed, it is known that the presence of oxygen-containing basic groups on the surface of activated carbon promotes the oxidative coupling of phenolic compounds and associated irreversible adsorption.[53] In this respect the highest adsorption capacity of AC could be related to the highest basic character, in agreement with the highest $pH_{pzc}$ value. Rather, no clear correlation was observed between the acid/base properties of the CNTs and their adsorption capacities, which substantially reflects the changes in the SAs of the samples (Table 1). Indeed, as a result of oxidation of the carbon surface, the lowering of the basic carbonyl-type groups, shown by the decrease of CO desorption in the range 973−1223 K (Figure 4b), and the increase in the amount of acid groups such as carboxylic acid (between 400−650 K in Figure 4a) that do not promote irreversible adsorption,[54] a decrease of the extent of carbon adsorption is expected. However, it cannot be ruled out that phenol groups, whose amount increased from $f_{3:1}$-CNTs to $f_{1:1}$-CNTs, as evidenced by the CO desorption in the 837−1023 K range in Figure 4b, could also promote the oxidative coupling[54] at such an extent, giving rise to the lack of a clear trend.

The removal rate of *p*-coumaric acid, $V$ (mol $g_{cat}^{-1}$ $min^{-1}$), calculated at 30 min of reaction and reported in Table 2, ranks in the order AC > p-CNTs > $f_{1:3}$-CNTs > $f_{3:1}$-CNTs > $f_{1:1}$-CNTs.

As shown in Table 2, the same order was maintained after subtraction of the carbon adsorption rate, $V_{ads}$ (mol $g_{cat}^{-1}$ $min^{-1}$), calculated for each catalyst from $C_{ads}$ (%) data assuming that carbon adsorption was completed within 30 min of contact time.


dx.doi.org/10.1021/ie200492g |*Ind. Eng. Chem. Res.* 2011, 50, 9043–9053

This result indicates that the observed sequence reflects the intrinsic oxidation activities of the catalysts.

No correlation can be drawn between the SAs of the samples and their catalytic activities, as demonstrated by the different activities of samples p-CNTs, $f_{3:1}$-CNTs, and $f_{1:1}$-CNTs (Table 2), which have similar SAs (194−196 $m^2/g$).

The performance of the samples was instead in line with the decreasing of the basic properties of the samples, in agreement with literature data on the importance of the basic sites of carbon materials for liquid-phase oxidation,[14,23,26] but for $f_{1:3}$-CNTs.

The most basic samples, with the highest $CO/CO_2$ ratios and $pH_{pzc}$ values, namely, AC and p-CNTs, were indeed the most active, and between them, AC was more active than p-CNTs because of the higher base character (see $CO/CO_2$ and $pH_{pzc}$ in Table 2).

The progressive lowering of the base character, as in the case of $f_{3:1}$-CNTs and $f_{1:1}$-CNTs, was accompanied by a decrease of the rate of *p*-coumaric acid removal, in agreement with the previous findings for the continuous CWAO of phenol over unmodified and $H_2O_2$-, $(NH_4)_2S_2O_8$-, $HNO_3$-, and HCl-modified activated carbons.[23] The lower steady phenol conversions found for the modified carbons with respect to the original are related to the destruction of the more active basic sites or the generation of no catalytically active new lactone and carboxylic groups over the carbon surface upon modification.[23]

The exception is the sample $f_{1:3}$-CNTs, which, notwithstanding its strongest acid character (i.e., the lowest $CO/CO_2$ ratio and $pH_{pzc}$ value), showed the highest rate of removal of *p*-coumaric acid among $f_{N:S}$-CNTs. The different behavior of $f_{1:3}$-CNTs could be due to their highest amount of sulfur-containing groups on the carbon surface, which, in agreement with previous findings,[51] can act as promoters.

For the sake of completeness, the influence of the iron present in the CNTs on their catalytic behavior is discussed. Analysis of the reaction mixture indicated that, for all samples, a very low amount of iron (Fe < 0.2 ppm) was leached. The homogeneous activity eventually arising from the presence of this amount of iron was evaluated by subjecting the liquid phase recovered after one catalytic cycle to a second cycle after elimination of the solid catalyst and addition of a proper amount of *p*-coumaric acid. The phenol conversion attained after 5 h was comparable to that obtained in the absence of catalyst (∼20%); therefore, it can be ruled out that $Fe^{2+}$ and/or $Fe^{3+}$ is responsible for the observed activity. However, although it cannot be ruled out that iron present in CNTs could act as a promoter for the reaction, as previously observed for iron ceria mixed oxide catalysts,[9] under the present metal content (3.4−5.9 wt % as iron oxide), its promoting effect, if any, seems to be less relevant for the catalytic activity than the acid/base character of the samples. This is suggested by the lowering of the *p*-coumaric acid removal rate from p-CNTs to $f_{3:1}$-CNTs (Table 2) with the lowering of basic character (i.e., $CO/CO_2$ ratio and $pH_{pzc}$ value), despite the similar iron content (5.9% and 5.5% as iron oxide). Further evidence of the main role exerted by the acid/base properties of the carbonaceous materials in the catalytic performance of CNTs is also demonstrated by the results obtained in the degradation of *p*-coumaric acid with $f_{3:1}$-CNTs thermally treated at 873 K for 1 h under He atmosphere (Figure 5b). As a result of thermal treatment, TPD analysis (not shown) indicated a decrease of $CO_2$ released in the range 400−750 K, where decomposition of carboxylic acid groups mainly occurs, whereas the amount of the more basic carbonyl functionalities, and thus the amount of CO released, remained almost unmodified. The consequence is that the $CO/CO_2$ ratio and $pH_{pzc}$ value increased with respect to those of the untreated sample from 2.7 to 4.1 and from 2.54 to 6.90, respectively, as did the rate of *p*-coumaric acid removal (from 1.5 to 2.4 mol $g_{cat}^{-1}$ $min^{-1}$).

In summary, the results show that AC and p-CNTs, thanks to their base character, showed the best performance toward the degradation of *p*-coumaric acid. Our results are in line with the expected promoting effect of the surface basicity mainly rising from the presence of carbonyl-type groups over the carbon surface.[14,23,26] In fact, it is generally accepted that basic surface groups play a major role in the catalytic activity of carbon materials because of their ability to generate oxygenated radicals.[14]

Functionalization of CNTs by nitric/sulfuric acid ratios 3:1 and 1:1 was found to be detrimental for their catalytic activity because of the lowering of the base character, as shown by the lowering of the $CO/CO_2$ ratio and $pH_{pzc}$ value (Table 2).

CNT oxidation with the most sulfuric acid-rich mixture (1:3) led to a sample with the highest activity among $f_{N:S}$-CNTs, despite having the highest acid character, likely because of the promoter effect exerted by the presence of the highest amount of added sulfur groups; however, catalyst stability was still very problematic.

The aspect related to the faster deactivation of $f_{N:S}$-CNTs with respect to the original sample is still not clear, although some consideration can be made. Taking into account the fact that the amount of carbon recovered from the spent samples (see $C_{ads}$ in Table 2) was similar to the amount recovered in the case of $f_{3:1}$-CNTs and $f_{1:1}$-CNTs, or even lower ($f_{1:3}$-CNTs) than that obtained over the highly active p-CNTs, and that the surface area reduction after reaction (see $SA_{AR}$ in Table 1) also occurred to similar extents for p-CNTs and $f_{N:S}$-CNTs these changes, cannot satisfactorily explain the deactivation observed for $f_{N:S}$-CNTs (Figure 5a), at least for $f_{1:3}$-CNTs. Indeed, although, in the case of $f_{3:1}$-CNTs and $f_{1:1}$-CNTs, it can be speculated that, despite the similarity in the values of $C_{ads}$ with respect to p-CNTs, the complete loss of activity of the former might be due to the further diminishing of the active sites by carbon coverage, in the case of $f_{1:3}$-CNTs, instead, it was found that this explanation is not totally reasonable as the activity of the sample was as high as that measured for p-CNTs and the amount of adsorbed carbon was lower. Therefore, other effect should be considered.

In an article dealing with the continuous CWAO of phenol over unmodified and $H_2O_2$-, $(NH_4)_2S_2O_8$-, $HNO_3$-, and HCl-modified charcoal by Santiago et al.,[23] some indications suggest that modification of the surface group distribution during the reaction might play a role in catalyst deactivation. They found that, after an initial adsorption period (apparent 100% phenol conversion), phenol oxidation started and conversion dropped until it reached a constant value. The steady-state phenol conversion over unmodified charcoal was higher than that measured over the modified sample. The phenol decrease was more severe for modified than unmodified carbon indicating a higher deactivation. Phenol adsorption, that last simultaneously with its oxidation and is lower for modified than for unmodified charcoal, and the loss of BET surface area during reaction do not seem the only critical parameters negatively affecting the catalytic performance observed.[23]

As previously mentioned, the lowering of the steady phenol conversion for the modified carbon was related to the destruction of the more active basic sites or the generation of no catalytically

active new lactone and carboxylic groups over the carbon surface upon modification treatment, whereas no explanation was given for the catalyst deactivation. However, in the same article, it was reported that the spent unmodified and modified charcoal, recovered after 50 h of reaction, showed a weight change, monitored by means of TGA under He, notably greater than that of the fresh catalysts. Although the authors did not provide for an identification of the species released during TGA,[23] they suggested that the increase of the weight loss for the spent catalyst was due to the new carboxylic, lactone, and probably some phenolic groups introduced onto the carbon surface by continuous oxygen attack[14] and by the cracking of hydrocarbon adsorbed species.[23] Among the catalysts investigated, the highest weight loss was observed for the spent modified charcoal, whereas the unmodified carbon showed the lowest mass reduction, and it was concluded that the unmodified carbon mainly conserved their original surface group distribution and, therefore, the original activity.[23]

Although no mention is given to the possible role of the newly introduced groups on the observed deactivation, it was found that the greater the change in surface group distribution, such in the case of modified charcoal, the higher drop of conversion.

Clear evidence of the modification of the surface group distribution and its role in the catalytic behavior was reported by Pereira et al.[55] in a study of the oxidative dehydrogenation (ODH) of ethylbenzene over activated carbon. Upon a detailed study in which the temporal evolution of CO and $CO_2$ desorbed from the catalyst, the amount of coke deposited, and the ethylbenzene conversion with the time on stream up to 4320 min were monitored simultaneously, it was demonstrated that oxygenated groups formed during the run do not intervene in the reaction and are not the main cause of the deactivation.

In the present study, preliminary TPD analysis of spent catalysts (not shown) suggested that catalyst surface modifications occurred during the run. However, for a deeper comprehension of their role in catalytic performance, research is ongoing to evaluate the temporal evolution of the textural and surface properties of samples, in agreement with the method already reported for the study of deactivation for ODH of ethylbenzene.[55]

The catalyst efficiency toward the removal of the organic carbon, evaluated from TOC analysis, is shown in Figure 6.

AC and p-CNTs exhibited the highest efficiency, showing, after 5 h, TOC abatements, ΔTOC (%), of 85.3% and 87.6%, respectively. Between the two, AC removed 80% of the initial TOC already after 50 min of reaction, whereas p-CNTs reached this value at longer contact time (80 min). $f_{N:S}$-CNTs showed a lower organic compound removal capacity, in agreement with its lower *p*-coumaric acid degradation (Figure 5a). However, although the amounts of *p*-coumaric acid eliminated after 5 h by $f_{N:S}$-CNTs samples were similar (Figure 5a), $f_{3:1}$-CNTs and $f_{1:1}$ CNTs allowed higher TOC abatements to be obtained than $f_{1:3}$-CNTs (Figure 6).

These results suggest that, the introduction of sulfur groups onto the carbon surface in a proper amount to act as an activity promoter, as in the $f_{1:3}$-CNTs sample, favors the degradation of *p*-coumaric acid mainly into lower-molecular-weight compounds.

The mineralization effectiveness of the catalysts, $C_{CO_2}$ (%), which represents the extent to which elimination of organic carbon from the solution occurred through complete oxidation to the less harmful $CO_2$, was evaluated by applying the following mass balance equation

$$\Delta TOC\ (\%) = C_{CO_2}\ (\%) + C_{ads}\ (\%)$$

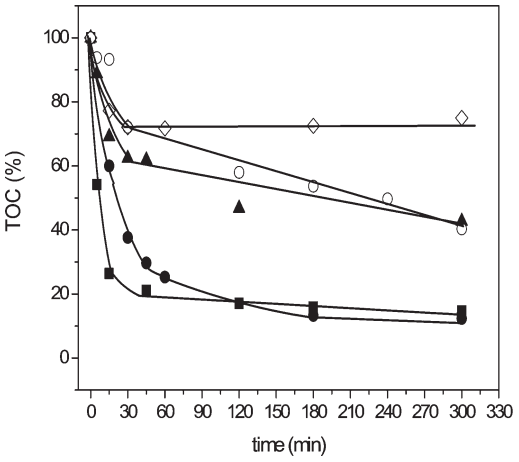


**Figure 6.** TOC abatement during CWAO, at 353 K in air at 2 MPa, over (■) AC, (●) p-CNTs, (▲) $f_{3:1}$-CNTs, (○) $f_{1:1}$-CNTs, and (◇) $f_{1:3}$-CNTs.

which indicates that the main routes for the elimination of organic carbon from the solution (ΔTOC%) are mineralization, $C_{CO_2}$ (%), and adsorption onto the catalyst, $C_{ads}$ (%).

The prevalence of the mineralization contribution is of importance for the selection of a good catalyst for pollutant removal and, moreover, guarantees an improvement in the catalyst lifetime, in the absence of factors other than adsorption that can compromise the catalyst performance, and reduces the energy- and time-consuming regeneration processes required for catalyst reuse.

As reported in Table 2, p-CNTs showed the highest mineralization efficiency, with the value of $C_{CO_2}$ (82.6%), being almost 94% with respect to ΔTOC (%). A lower $C_{CO_2}$ (%) value of 71.2% was instead found for AC, which corresponds to 83% of ΔTOC (%). $f_{N:S}$-CNTs obviously exhibited lower values of $C_{CO_2}$ (%), in accordance with their low ΔTOC (%) values (Figure 6). However, the contribution to ΔTOC (%) ranged between 87% and 91%, higher than the 83% found for AC.

It is known that addition of iron oxide to AC strongly improves the mineralization effectiveness in the oxidation of phenol,[56] so the possibility that iron impurities present in CNTs (Table 1) are responsible for the highest mineralization observed cannot be ruled out. Although their accessibility to organics should be very limited, being mostly encapsulated within the graphitic structure, the detection of a low amount of iron cations (<0.2 ppm) in the reaction solution suggests that some exposed sites were present. The highest amount of adsorbed carbon was measured over AC compared to CNTs, which, in turn, caused a significant lowering of the effective surface area during the reaction (see $SA_{AR}$ values in Table 1), so a decrease of the active sites could also be responsible for the lower mineralization efficiency.

In conclusion, it is worth noting that, among the catalysts investigated, AC and p-CNTs catalysts exhibited the best catalytic performance, in terms of *p*-coumaric acid removal (Figure 5a) and TOC abatement (Figure 6); however, p-CNTs allowed the highest mineralization efficiency to be achieved. A comparative analysis of the results obtained in the present work with literature data clearly reveals that AC and p-CNTs are promising heterogeneous catalysts for the CWAO of *p*-coumaric acid, under mild conditions.

With respect to $CeO_2$, one of the most efficient catalytic system in the CWAO of *p*-coumaric acid under the same conditions as

used in the present work ($P$ = 2 atm, $T$ = 353 K, *p*-coumaric acid concentration = 4.5 mM),[12] AC and p-CNTs showed higher ΔTOC values of 85.3% and 87.6% compared to 78%, as well as the highest mineralization effectiveness, 71.2% and 82.6% compared to 39%. The catalytic performances of AC and p-CNTs were even superior to that shown by $Pt/CeO_2$ catalysts.[12] Although carbonaceous samples and $Pt/CeO_2$ exhibited close ΔTOC values, the former had a dramatically higher mineralization efficiency, 71.2% and 82.6% compared to 55%.

Finally, it should be mentioned that AC and p-CNTs showed higher mineralization effectiveness than the best performing $Ru/TiO_2$ and $Ru/ZrO_2$ catalysts tested under more severe reaction conditions ($P$ = 5 MPa, $T$ = 413 K)[11] than those used in the present work.

Indeed, with Ru catalysts, mineralization of only 70% was achieved, whereas AC and p-CNTs allowed similar (71.2% for AC) or even superior (82.6% for p-CNTs) performance to be achieved under milder conditions.

## 4. CONCLUSIONS

The results of the present study showed that carbonaceous materials such as AC and p-CNTs, the latter prepared by CCVD over iron-supported catalysts, are efficient catalysts for the CWAO of *p*-coumaric acid under mild conditions (in air, $T$ = 353 K, $P$ = 2 MPa), allowing almost complete *p*-coumaric acid removal to be achieved at 5 h of contact time with a ΔTOC values of 85.3% for AC and 87.6% for p-CNTs

p-CNTs showed the highest mineralization effectiveness, as the amount of carbon removed through oxidation to $CO_2$ was 82.6%, whereas in the case of AC, only 71.2% of the initial carbon content was mineralized. The highest mineralization effectiveness shown by p-CNTs was likely promoted by the presence of encapsulated iron impurities from the CCVD process that cannot be removed under the mild postsynthesis purification step.

Liquid-phase treatment of p-CNTs by nitric/sulfuric acid mixtures with different volume ratios caused a progressive downgrade of the crystalline quality of CNTs, an enhancement of the acid character of the carbon surface, and an increase of the sulfur groups introduced as the sulfuric acid concentration increased, which is detrimental to catalyst stability under the reaction conditions, as demonstrated by the significant deactivation occurring after 30 min of reaction.

The catalytic activity of carbonaceous samples, evaluated within 30 min of reaction, strongly depends on the acid/base properties, decreasing with the diminishing of the base character of the carbon surface, except for $f_{1:3}$-CNTs, which contained the highest amount of sulfur groups on the surface, which can act as promoters.

Finally, because of their improved performance compared to metal oxide and metal-supported catalysts reported in the literature, AC and p-CNTs are very promising catalysts for the CWAO of *p*-coumaric acid under mild conditions.

## AUTHOR INFORMATION

### Corresponding Author

*E-mail: cmilone@ingegneria.unime.it.

## ACKNOWLEDGMENT

The authors are grateful to Professor Francesco Arena that provided for TPD facilities.

## REFERENCES

(1) El Hadrami, A.; Belaqziz, M.; Hassni, M.; Hanifi, S.; Abbad, A.; Capasso, R.; Gianfreda, L.; El Hadrami, I. Physico-Chemical Characterization and Effects on Olive Oil Mill Waste Waters Fertirrigation on the Growth of Some Mediterranean Crops. *J. Agron.* **2004**, *3*, 247.

(2) Perez, J.; De la Rubia, T.; Moreno, E.; Martinez, J. Phenolic Content and Anti Bacterial Activity of Olive Oil Waste Waters. *Environ. Toxicol. Chem.* **1992**, *11*, 489.

(3) Capasso, R.; Evidente, A.; Schivo, L.; Orru, G.; Marchialis, M.; Cristinzio, G. Antibacterial Polyphenols from Olive Oil Mill Waste Waters. *J. Appl. Microbiol.* **1995**, *79*, 393.

(4) Bedoul, A.; Sindi, K.; Bensalah, N. Treatment of Refractory Organics Contained in Actual Agro-Industrial Waste Waters by $UV/H_2O_2$. *Clean* **2008**, *36*, 373.

(5) Rivas, F. J.; Beltran, F. J.; Gimeno, O. Treatment of Olive Oil Mill Waste Water by Fenton's Reagent. *J. Agric. Food. Chem.* **2001**, *49*, 1873.

(6) Salles, M. O.; Paixão, T. R. L. C.; Bertotti, M. Hydrogen Peroxide Monitoring in Photo-Fenton Reactions by Using a Metal Hexacyanoferrate Modified Electrode. *Int. J. Electrochem. Sci.* **2007**, *2*, 248.

(7) Minh, D. P.; Gallezot, P.; Azabou, S.; Sayadi, S.; Besson, M. Catalytic Wet Air Oxidation of Olive Oil Mill Effluents: 4. Treatment and Detoxification of Real Effluents. *Appl. Catal. B* **2008**, *84*, 749.

(8) Mantzavinos, D.; Hellenbrand, R.; Livingston, G.; Metcalfe, I. S. Catalytic Wet Oxidation of *p*-Coumaric Acid: Partial Oxidation Intermediates, Reaction Pathways and Catalyst Leaching. *Appl. Catal. B* **1996**, *7*, 379.

(9) Neri, G.; Pistone, A.; Milone, C.; Galvagno, S. Wet Air Oxidation of *p*-Coumaric Acid over Promoted Ceria Catalysts. *Appl. Catal. B* **2002**, *38*, 321.

(10) Perkas, N.; Pham Minh, D.; Gallezot, P.; Gedanken, A.; Besson, M. Platinum and Ruthenium Catalysts on Mesoporous Titanium and Zirconium Oxides for the Catalytic Wet Air Oxidation of Model Compounds. *Appl. Catal. B* **2005**, *59*, 121.

(11) Minh, D. P.; Gallezot, P.; Besson, M. Degradation of Olive Mill Effluents by Catalytic Wet Air Oxidation: 1. Reactvity of *p*-Coumaric Acid over Pt and Ru Supported Catalysts. *Appl. Catal. B* **2006**, *63*, 68.

(12) Milone, C.; Fazio, M.; Pistone, A.; Galvagno, S. Catalytic Wet Air Oxidation of *p*-Coumaric Acid on $CeO_2$, Platinum and Gold Supported on $CeO_2$ Catalysts. *Appl. Catal. B* **2006**, *68*, 28.

(13) Garcia-Araya, J. F.; Beltran, F. J.; Alvarez, P.; Masa, F. J. Activated Carbon Adsorption of Some Phenolic Compounds Present in Agro Industrial Waste Water. *Adsorption* **2003**, *9*, 107.

(14) Stüber, F.; Font, J.; Fortuny, A.; Bengoa, C.; Eftaxias, A.; Fabregat, A. Carbon Materials and Catalytic Wet Air Oxidation of Organic Pollutants in Waste Water. *Top. Catal.* **2005**, *33*, 3.

(15) Oliviero, L.; Barbier, J., Jr.; Duprez, D.; Guerrero-Ruiz, A.; Bachiller-Baeza, B.; Rodriguez-Ramos, I. Catalytic Wet Air Oxidation of Phenol and Acrylic Acid over Ru/C and Ru-$CeO_2$/C Catalysts. *Appl. Catal. B* **2000**, *25*, 267.

(16) Eugenia Suarez-Ojeda, M.; Stüber, F.; Fortuny, A.; Fabregat, A.; Carrera, J.; Font, J. Catalytic Wet Air Oxidation of Phenols Using Activated Carbon as Catalyst. *Appl. Catal. B* **2005**, *58*, 105.

(17) Eftaxias, A.; Font, J.; Fortuny, A.; Fabregat, A.; Stüber, F. Catalytic Wet Air Oxidation of Phenol Over Active Carbon Catalyst: Global Kinetic Modelling Using Simulated Annealing. *Appl. Catal. B* **2006**, *67*, 12.

(18) Serp, P.; Corrias, M.; Kalck, P. Carbon Nanotubes and Nanofibres in Catalysis. *Appl. Catal. A* **2003**, *253*, 337.

(19) Liu, Z. Q.; Maa, J.; Cui, Y. H.; Zhang, B. P. Effect of Ozonation Pretreatment on the Surface Properties and Catalytic Activity of Multi-Walled Carbon Nanotubes. *Appl. Catal. B* **2009**, *92*, 301.

(20) Rinaldi, A.; Zhang, J.; Mizera, J.; Girgsdies, F.; Wang, N.; Hamid, S. B. A.; Schögl, R. Facile Synthesis of Carbon Nanotube/Natural Bentonite Composies as a Stable Catalyst for Styrene Synthesis. *Chem. Commun.* **2008**, *48*, 6528.

(21) Yang, S.; Li, X.; Zhu, W.; Wang, J.; Descorme, C. Catalytic Activity, Stability and Structure of Multi-Walled Carbon Nanotubes in the Wet Air Oxidation of Phenol. *Carbon* **2008**, *46*, 445.

(22) Liu, Z. Q.; Ma, J.; Cui, Y. H.; Zhao, L.; Zhang, B. P. Influence of Different Heat Treatments on the Surface Properties and Catalytic Performance of Carbon Nanotube in Ozonation. *Appl. Catal. B* **2010**, *101*, 74.

(23) Santiago, M.; Stüber, F.; Fortuny, A.; Fabregat, A.; Font, J. Modified Activated Carbon for Catalytic Wet Air Oxidation of Phenol. *Carbon* **2005**, *43*, 2134.

(24) Rodriguez Reinoso, F. The Role of Carbon Materials in Heterogeneous Catalysis. *Carbon* **1998**, *36*, 159.

(25) Su, D. S.; Zhang, J.; Frank, B.; Thomas, A.; Wang, X.; Paraknowitsch, J.; Schlögl, R. Metal Free Heterogeneous Catalysis for Sustainable Chemistry. *ChemSusChem* **2010**, *3*, 169.

(26) Figueiredo, J. L.; Pereira, M. F. R. The Role of Surface Chemistry in Catalysis. *Catal. Today* **2010**, *150*, 2.

(27) Donato, M. G.; Galvagno, S.; Lanza, M.; Messina, G.; Milone, C.; Piperopoulos, E.; Pistone, A.; Santangelo, S. Influence of Carbon Source and Fe-Catalyst Support on the Growth of Multi-Walled Carbon Nanotubes. *J. Nanosci. Nanotechnol.* **2009**, *9*, 3815.

(28) Lafuente, E.; Callejas, M. A.; Sainz, R.; Benito, A. M.; Maser, W. K.; Sanjuán, M. L.; Saurel, D.; De Teresa, J. M.; Martínez, M. T. The Influence of Single-Walled Carbon Nanotube Functionalization on the Electronic Properties of Their Polyaniline Composites. *Carbon* **2008**, *46*, 1909.

(29) Zhao, X.; Ando, Y.; Qin, L.-C.; Kataura, H.; Maniwa, Y.; Saito, R. Multiple Splitting of G-band Modes from Individual Multiwalled Carbon Nanotubes. *Appl. Phys. Lett.* **2002**, *81*, 2550.

(30) Goncalves, A. G.; Figueiredo, J. L.; Órfão, J. J. M.; Pereira, M. F. R. Influence of the Surface Chemistry of Multi-Walled Carbon Nanotubes on Their Activity as Ozonation Catalysts. *Carbon* **2010**, *48*, 4369.

(31) Rivera-Utrilla, J.; Bautista-Toledo, I.; Ferro-García, M.; Moreno-Castilla, C. Activated Carbon Surface Modifications by Adsorption of Bacteria and Their Effect on Aqueous Lead Adsorption. *J. Chem. Technol. Biotechnol.* **2001**, *76*, 1209.

(32) Santangelo, S.; Messina, G.; Donato, M. G.; Lanza, M.; Milone, C.; Pistone, A. Low-frequency Raman Study of Hollow Multi-Walled Nanotubes Grown by Fe Catalyzed Chemical Vapor Deposition. *J. Appl. Phys.* **2006**, *100*, 104311–1.

(33) Porro, S.; Musso, S.; Vinante, M.; Vanzetti, L.; Anderle, M.; Trotta, F.; Tagliaferro, A. Purification of Carbon Nanotubes Grown by Thermal CVD. *Physica E* **2007**, *37*, 58.

(34) Kouklin, N.; Tzolov, M.; Straus, D.; Yin, A.; Xu, J. Infrared Absorption Properties of Carbon Nanotubes Synthesized by Chemical Vapour Deposition. *Appl. Phys. Lett.* **2004**, *85*, 4463.

(35) Xia, W.; Jin, C.; Kundu, S.; Muhler, M. A Highly Efficient Gas Phase Route for the Oxygen Functionalization of Carbon Nanotubes Based on Nitric Acid Vapor. *Carbon* **2009**, *47*, 919.

(36) Osswald, S.; Havel, M.; Gogotsi, Y. Monitoring Oxidation of Multiwalled Carbon Nanotubes by Raman Spectroscopy. *J. Raman Spectrosc.* **2007**, *38*, 728.

(37) Chen, C. C.; Chen, C. F.; Chen, C. M.; Chuang, F. T. Modifications of Multi-Walled Carbon Nanotubes by Microwave Digestion Method as Electrocatalyst Supports for Direct Methanol Fuel Cell Applications. *Electrochem. Commun.* **2007**, *9*, 159.

(38) Yang, C.; Hu, X.; Wang, D.; Dai, C.; Zhang, L.; Jin, H.; Agathopoulos, S. Ultrasonically Treated Multi-Walled Carbon Nanotubes (MWCNTs) as PtRu Catalyst Supports for Methanol Electro Oxidation. *J. Power Sources* **2006**, *160*, 187.

(39) Ferrari, A. C.; Robertson, J. Interpretation of Raman Spectra of Disordered and Amorphous Carbon. *Phys. Rev. B* **2000**, *61*, 14095.

(40) Wang, Z.; Huang, X.; Xue, R.; Chen, L. Aid of Raman Spectroscopy in Diagnostics of MWCNT Synthesised by Fe-Catalysed CVD. *J. Appl. Phys.* **1998**, *84*, 227.

(41) Kim, Y. A.; Hayashi, T.; Osawa, K.; Dresselhaus, M. S.; Endo, M. Annealing Effect on Disordered Multi-Walled Carbon Nanotubes. *Chem. Phys. Lett.* **2003**, *380*, 319.

(42) Dresselhaus, M. S.; Dresselhaus, G.; Saito, R.; Jorio, A. Raman Spectroscopy of Carbon Nanotubes. *Phys. Rep* **2005**, *409*, 47.

(43) Thomsen, C.; Reich, S. Double Resonant Raman Scattering in Graphite. *Phys. Rev. Lett.* **2000**, *85*, 5214.

(44) Donato, M. G.; Faggio, G.; Galvagno, S.; Lanza, M.; Messina, G.; Milone, C.; Piperopoulos, E.; Pistone, A.; Santangelo, S. Influence of Gas-Mixture Composition on Yield, Purity and Morphology of Carbon Nanotubes Grown by Catalytic Isobutane Decomposition. *Diamond Relat. Mater.* **2009**, *18*, 360.

(45) Chiang, Y. C.; Lin, W. H.; Chang, Y. C. The Influence of Treatment Duration on Multi-Walled Carbon Nanotubes Functionalized by $H_2SO_4/HNO_3$ Oxidation. *Appl. Surf. Sci.* **2011**, *257*, 2401.

(46) Silvestre-Albero, A.; Silvestre-Albero, J.; Sepúlveda-Escribano, A.; Rodríguez-Reinoso, F. Ethanol Removal Using Activated Carbon: Effect of Porous Structure and Surface Chemistry. *Microporous Mesoporous Mater.* **2009**, *120*, 62.

(47) Moreno-Castilla, C.; Lopez-Ramon, M. V.; Carrasco-Marın., F. Changes in Surface Chemistry of Activated Carbon by Wet Oxidation. *Carbon* **2000**, *38*, 1995.

(48) Erhan Aksoylu, A.; Madalena, M.; Freitas, A.; Fernando, M.; Pereira, R.; Figueiredo, J. L. The Effects of Different Activated Carbon Supports and Support Modifications on the Properties of Pt/AC Catalysts. *Carbon* **2001**, *39*, 175.

(49) Figueiredo, J. L.; Pereira, M. F. R.; Freitas, M. M. A.; Órfão, J. J. M. Modification of the Surface Chemistry of Activated Carbons. *Carbon* **1999**, *37*, 1379.

(50) Figueiredo, J. L.; Pereira, M. F. R.; Freitas, M. M. A.; Órfão, J. J. M. Characterization of Active Sites on Carbon Catalysts. *Ind. Eng. Chem. Res.* **2007**, *46*, 4110.

(51) Gomes, H. T.; Miranda, S. M.; Sampaio, M. J.; Silva, A. M. T.; Faria, J. L. Activated Carbons Treated with Sulphuric Acid: Catalysts for Catalytic Wet Peroxide Oxidation. *Catal. Today* **2010**, *151*, 153.

(52) Terzyk, A. P. Further Insights Into the Role of Carbon Surface Functionalities in the Mechanism of Phenol Adsorption. *J. Colloid Interface Sci.* **2003**, *268*, 301.

(53) Vidic, R. D.; Tessmer, C. H.; Uranowski, L. J. Impact of Surface Properties of Activated Carbons on Oxidative Coupling of Phenolic Compounds. *Carbon* **1997**, *35*, 1349.

(54) Grant, T. M.; King, C. J. Mechanism of Irreversible Adsorption of Phenolic Compounds by Activated Carbons. *Ind. Eng. Chem. Res.* **1990**, *29*, 264.

(55) Pereira, M. F. R.; Órfão, J. J. M.; Figueiredo, J. L. Oxidative Dehydrogenation of Ethylbenzene on Activated Carbon Catalysts 3. Catalyst Deactivation. *Appl. Catal. A* **2001**, *218*, 307.

(56) Quintanilla, A.; Menéndez, N.; Tornero, J.; Casas, J. A.; Rodríguez, J. J. Surface Modification of Carbon-Supported Iron Catalyst During the Wet Air Oxidation of Phenol: Influence on Activity, Selectivity and Stability. *Appl. Catal. B* **2008**, *81*, 105.